Fish and Shellfish Immunology 84 (2019) 304–311

Contents lists available at ScienceDirect

Fish and Shellfish Immunology

journal homepage: www.elsevier.com/locate/fsi

Full length article

# Ark shell *Scapharca broughtonii* hemocyte response against *Vibrio anguillarum* challenge

Liqing Zhou[b,c], Dan Zhao[b,d], Biao Wu[b,c], Xiujun Sun[b,c], Zhihong Liu[b,c], Feng Zhao[a], Zhenming Lv[e], Aiguo Yang[b,c,*], Qing Zhao[b,d], Gaowei Zhang[b,d], Chunyan Ma[a]

[a] Key Laboratory of East China Sea, Oceanic Fishery Resources Exploitation and Utilization, Ministry of Agriculture, Shanghai, 20090, PR China
[b] Key Laboratory of Sustainable Development of Marine Fisheries, Ministry of Agriculture, Yellow Sea Fisheries Institute, Chinese Academy of Fishery Sciences, Qingdao, 266071, PR China
[c] Laboratory for Marine Fisheries Science and Food Production Processes, Qingdao National Laboratory for Marine Science and Technology, Qingdao, 266071, PR China
[d] College of Fisheries and Life Science, Shanghai Ocean University, Shanghai, 20090, PR China
[e] College of Marine Science and Technology, Zhejiang Ocean University, Zhoushan, 316022, PR China

ARTICLE INFO

*Keywords:*
*Scapharca broughtonii*
Hemocyte
Lysozyme
*Vibrio anguillarum*
Red blood cell
White blood cell
Thrombus cell

ABSTRACT

*Scapharca broughtonii* is one of the most important Arcidae aquaculture species in the Asia-Pacific region. We aimed to investigate the immune responses of hemocytes from ark shell *S. broughtonii* hemolymph against pathogens. Hemocyte ultrastructure and immunological activity in response to *Vibrio anguillarum* challenge were observed by scanning and transmission electron microscopy. Before ultrastructure observation, we used the API ZYM semi-quantitative kit to evaluate the levels of hydrolytic enzymes in the plasma and hemocytes following *V. anguillarum* infection. An enzyme-linked immunosorbent assay kit was used to investigate the variation in the lysozyme activity and hemocytes following bacterial infection. The results showed that hemocytes were the main defense cells against bacterial infection, whereas plasma played a role in the transport and support of hemocytes. It was presumed that an important function of lysozymes and hydrolytic enzymes in lysosomes was for bacterial digestion. Three major types of hemocytes were observed, namely, red blood cells (RBCs), white blood cells (WBCs), and thrombocytes (TCs). Scanning electron microscopy showed that the normal RBCs appeared pie-shaped with 10 μm diameter and 4 μm central thickness, whereas WBCs were spherical in shape with varying sizes, 4–8 μm diameter, and included small lymphocytes. TCs were long, spindle-shaped, and 12–20 μm in length. The cell membrane surface was smooth and even for all cells before pathogen challenge. Under transmission electron microscopy, RBCs displayed a limited ability to devour and digest bacteria adherent to the cell surface following infection. Many hemoglobin particles were observed in the RBC cytoplasm. WBCs were very active against bacterial invasion and showed a strong ability to digest and decompose infected and wrapped *V. anguillarum* through phagocytosis and lysosome fusion. Digestive vacuoles rapidly became transparent and were thought to contain increasing quantities of pathogen-induced lysozymes. WBCs that devoured pathogenic bacteria were prone to deformation as well as adhesion to each other. TCs were rich in endoplasmic reticulum (ER) content in their cytoplasm and were widely connected in a net-shaped structure. Mitochondria in TCs formed clusters upon invasion of *V. anguillarum* in the hemolymph. TCs disintegrated to release the ER into the plasma to form a mesh that facilitated clotting. The ability of circulating hemocytes to quickly modify their morphologies and stainability suggests that *S. broughtonii* is endowed with highly dynamic hemocyte populations capable of coping with environmental changes and rapidly growing pathogens.

## 1. Introduction

The circulating hemocytes from *Scapharca broughtonii* play a central role in innate immunity. Three types of hemocytes are known, namely, red blood cells (RBCs), white blood cells (WBCs), and thrombocytes (TCs). These classifications resemble those of vertebrate hemocytes that exert systemic immunologic defense mechanisms against mass pathogen invasion into the body of ark shells [1]. These hemocyte classes

* Corresponding author. Key Laboratory of Sustainable Development of Marine Fisheries, Ministry of Agriculture, Yellow Sea Fisheries Institute, Chinese Academy of Fishery Sciences, Qingdao, 266071, PR China.
*E-mail address:* yangag@ysfri.ac.cn (A. Yang).

https://doi.org/10.1016/j.fsi.2018.09.039
Received 10 June 2018; Received in revised form 24 August 2018; Accepted 12 September 2018
Available online 13 September 2018

are functionally and morphologically essential and vary from the common classes based on granule number and size, as assessed via light microscopy and transmission electron microscopy (TEM) [2]. Three types of anticoagulants were found to effectively prevent ark shell blood from clotting and play an important role in hemocyte immune function [3]. We have studied blood cell morphological changes in *S. broughtonii* hemolymph after immunostimulation with pathogenic *Vibrio anguillarum* using two regular anticoagulants under an oil-immersion lens of a Leica microscope [4]. In addition, we have studied the antibacterial activity of hemoglobin [5], ferritin [6], manganese superoxide dismutase (MnSOD) [7], and catalase [8] in ark shell *S. broughtonii*. However, the cellular immune response of *S. broughtonii* to pathogenic organisms is still unstudied.

Ark shell *S. broughtonii* is an economically and ecologically popular aquaculture species in some East Asian countries, such as China, Korea, and Japan. Blood in most bivalves is colorless, although clams have red blood owing to the presence of RBCs and hemoglobin, which has an unusual subunit assembly similar to that observed in most vertebrate hemoglobins [9]. *S. broughtonii* natural resources have suffered from severe damage, mainly owing to over-exploitation, habitat loss, and environmental stress [10–12]. Pathogenic microorganisms often expand in seawater and deteriorate the ecological environment. However, studies exploring the antibacterial mechanism of hemocytes are still lacking.

In this study, we aimed to observe the ark shell *S. broughtonii* hemocyte response after *V. anguillarum* challenge for the better understanding of its stronger antibacterial ability in comparison with other bivalves and for the evaluation of the hemocyte immune functions.

## 2. Materials and methods

### 2.1. Animals

Healthy *S. broughtonii* specimens were selected from their habitats surrounding Qingdao City in Shandong Province, China. A total of 50 nearly 2-year-old ark shells, with an average shell length of 49.5 ± 4.7 mm and average body weight of 39.75 ± 9.8 g, were reared in two 50-L plastic tanks with fresh water set at 20 ± 2 °C. All animals were daily fed with cultured unicellular algae for at least seven days to ensure that they were healthy.

### 2.2. Bacterial immune stimulation and hemolymph sampling

All solutions used in this study were prepared with commercially available chemicals and reagents. The MAS (Modified Alserver's Solution) anticoagulant contained 20.8 g $L^{-1}$ of glucose, 8 g $L^{-1}$ of sodium citrate, 3.36 g $L^{-1}$ of ethylenediaminetetraacetic acid (EDTA), and 22.5 g $L^{-1}$ of sodium chloride (NaCl). Physiological saline (0.9%) contained 0.9 g of NaCl in 100 mL of distilled water. The 2611E marine culture medium comprised 0.05 g of yeast extract and 0.25 g of peptone in 50 mL of filtered seawater.

All of these solutions were sterilized in an autoclave. Gram-negative *V. anguillarum* were cultured in 2611E medium at 28 °C in a shaking bath for approximately 24 h. Cultured bacteria were diluted to $2 \times 10^8$ colony-forming units (CFU)·$mL^{-1}$ with physiological saline.

We injected *V. anguillarum* (0.1 mL) into the axe foot of 36 *S. broughtonii* specimens. The treated animals were reared separately from six control animals treated as the 0 h group. At 4, 8, 12, 24, 28, and 48 h post-injection, about 0.5 mL of hemolymph was collected from the anterior adductor muscle sinusoid of six individuals using disposable 1-mL syringes containing 0.5 mL MAS along with the six control individuals. Hemolymph samples were divided into three groups; one group was used for semi-quantitative analysis of enzymatic activity and the other for quantitative analysis of lysozyme activity. The last group was immersed into a fixative solution for electron microscopic observation.

### 2.3. Semi-quantitative analysis of enzymatic activity

The API ZYM semi-quantitative commercial chromogenic enzymatic kit (bioMérieux, France) was used to evaluate the level of enzymatic activity in the plasma and hemocytes in response to *V. anguillarum*, according to the manufacturer's guidelines. A sample of $2 \times 10^6$ hemocytes was then centrifuged (560 × *g* for 10 min) to separate the plasma and cells. Hypotonic cells were resuspended in 1 mL of distilled water, and 65 μL of this suspension or plasma was loaded in each well of a plate containing the substrates for each enzyme reaction. After 4 h of incubation at 37 °C, the enzyme activity was assessed using kit reagents [13]. In the treated group, several clams showed signs of a sluggish response to external disturbances, and their axe feet did not fully retract inside their shells, we named them 'diseased clams'. Hemolymph from two diseased ark shells was obtained for comparison. Among the previously mentioned 36 sample specimens, the groups treated for 4, 8, 24, and 28 h were selected for semi-quantitative analysis of enzymatic activity.

### 2.4. Quantitative analysis of lysozyme activity

An enzyme-linked immunosorbent assay (ELISA) kit (Shanghai Jianglai Biotech Ltd., Shanghai, China) was used to investigate variations in the lysozyme activity of hemocytes post-injection, according to the manufacturer's guidelines. The kit had a rabbit polyclonal antibody to the full length native lysozyme protein (purified) corresponding to the chicken lysozyme, which was a purified lysozyme from chicken egg white. The groups treated at 4, 12, 24, and 48 h were selected for the quantitative analysis of lysozyme activity. A sample of $2 \times 10^6$ hemocytes was centrifuged (560 × *g* for 10 min) to eliminate the supernatant. Hemocytes were then resuspended in 0.5 mL of 0.01 M phosphate-buffered saline (PBS; pH 7.2–7.4) and subjected to grinding in an ice bath to damage cells and release the intracellular components. Samples were centrifuged (560 × *g* for 20 min), and 50 μL of the supernatant and other required reagents were added to each test well of a plate containing the embedded antibody. After 1 h of incubation at 37 °C, 50 μL of stop solution was added to each well to stop the reaction. The blank well was considered as zero, and the absorbance was read at a 450 nm wavelength within 15 min from the addition of the stop solution. The enzyme activity was calculated based on a standard curve with the standard density, absorbance value, and dilution factor.

### 2.5. Electron microscopy

Groups incubated for 0, 4, 8, 12, and 28 h were selected for electron microscopy observation. Approximately 400 μL of hemolymph samples (about $2 \times 10^6$ hemocytes) were added into two sterile plastic 1.5-mL Eppendorf tubes filled with 200 μL of fixative (4% paraformaldehyde, 2.5% glutaraldehyde, and 0.05 M Tris dissolved in 500 mL of filtered seawater, pH 7.2) for use for scanning electron microscopy (SEM) and TEM. After 1.5 h fixation, the hemocytes were layered and settled to the bottom of the tube; the supernatant was carefully washed with a pipettor. Fixative was then replaced, and the samples were stored in a 4 °C refrigerator. The upper layer hemocytes of natural settlement contained all cell types; therefore, we retrieved the upper-middle-layer cells for electron microscopy, reducing dramatically the observation number of red blood cells and increasing relatively the observation number of white blood cells and thrombocytes. After rinsing thrice with 0.2 M PBS (pH 7.2), the hemocytes were fixed with 1% osmium tetroxide ($OsO_4$) for 1 h on ice. The cells were dehydrated with a series of ethanol (EtOH) solutions, subjected to critical-point drying, ion sputter-coated with gold (Hitachi, Tokyo, Japan), and viewed with an SEM (Hitachi S−3000N, Tokyo, Japan). The hemocyte pellets obtained were washed in 0.2 M PBS (pH 7.2), post-fixed in 1% $OsO_4$ in the same buffer, serially dehydrated in EtOH, and embedded via propylene oxide in Embed 812/Araldite. Ultra-thin sections were cut using a diamond knife on a


**Fig. 1.** API ZYM test of plasma and hemocytes in normal and 4, 8, 24, and 28 h groups with two diseased individuals for comparison. Normal, healthy ark shell without *Vibrio anguillarum* infection; 4, 8, 24, and 28 h, ark shells infected with *V. anguillarum* for approximately 4, 8, 24, and 28 h, respectively. Diseased 1 and 2, unhealthy individuals; No., number of test wells containing the substrates for each enzyme reaction. The enzymes used are listed below. 1. Control; 2. Alkaline phosphatase; 3. Esterase (C4); 4. Lipase esterase (C8); 5. Lipase (C14); 6. Leucine arylamidase; 7. Valine arylamidase; 8. Cystine arylamidase; 9. Trypsin; 10. α-chymotrypsin; 11. Acid phosphatase; 12. Naphthol-AS-BI-phosphohydrolase; 13. α-galactosidase; 14. β-galactosidase; 15. β-glucuronidase; 16. α-glucosidase; 17. β-glucosidase; 18. *N*— acetyl-β-glucosaminidase; 19. α-mannosidase; 20. β-fucosidase.

microtome. Sections were dried onto copper grids and stained with uranyl acetate and lead citrate [14]. Finally, sections were viewed via TEM (Hitachi HT7700, Tokyo, Japan).

## 3. Results

### 3.1. API ZYM test

Activity levels of 19 hydrolytic enzymes in clam hemocytes and plasma are shown in Fig. 1. Of these, alkaline phosphatase, esterase (C4), leucine arylamidase, valine arylamidase, acid phosphatase, naphthol-AS-BI-phosphohydrolase, β-galactosidase, β-glucuronidase, *N*-acetyl-β-glucosaminidase, and β-fucosidase showed high activity levels. Other enzymes were undetected or detected only at very low levels. Enzyme activity levels failed to change through bacterial invasion in the plasma. While the 8 and 24 h groups of hemocyte suspension showed characteristics similar to those observed for the two diseased groups, the 4 and 28 h groups of hemocyte suspension showed the same characteristics as the normal group.

### 3.2. Lysozyme

Variations in hemocyte lysozyme activity with bacterial immune stimulation determined by ELISA are shown in Fig. 2. In the 0 and 4 h groups, lysozyme activity was maintained at low levels, but the activity increased in the 12 h group. Levels of lysozymes peaked in the 24 h group, but the values greatly fluctuated between individuals. The lysozyme activity then decreased in the 48 h group, but it was still higher than that in the control group.

### 3.3. Scanning electron microscopy

Morphological characteristics of different types of hemocytes were observed under SEM. The membrane surfaces of all cells were smooth and even before pathogen challenge.

#### 3.3.1. Ultrastructure of healthy clam hemocytes

(1) Red blood cells

Normal RBCs appeared pie-shaped with a 10-μm diameter, 4-μm central thickness, and 0.6-μm edge thickness (Fig. 3a); 70–80% of hemocytes were RBCs.

(2) White blood cells

Normal WBCs were spherical in shape with varying sizes and a diameter of 4–8 μm (Fig. 3a). Small WBCs were usually lymphocytes (Fig. 3b). Nearly 15% of hemocytes were WBCs.

(3) Thrombocytes

Thrombocytes (TCs) were long, spindle-shaped, 12–20 μm in length, and had a single thick and thin end (Fig. 3c and d). Only 5–10% of hemocytes were TCs.

#### 3.3.2. Hemocyte ultrastructure response to bacterial invasion

(1) Morphological changes in the ultrastructure of RBCs and TCs

Bacteria were found in the hemolymph 4 h post-injection in the axe foot muscle. RBCs initially displayed bacterial adherence, but no obvious change in cell morphology was observed (Fig. 4a). At 8 h post *V. anguillarum* infection, RBCs showed passive phagocytosis of *V. anguillarum* that appeared as warts or dents on the surface of the cell membrane (Fig. 4b). The TC cell membrane surface became extremely rough and appeared stretched or loose post-infection (Fig. 4c).

(2) Morphological changes in the ultrastructure of WBCs

Leukocyte response to *V. anguillarum* invasion was intense, resulting in deformed spherical white cells, stretched pseudopodia, and *V. anguillarum* devoured in an amoeboid-like motion (Fig. 5a and b). These changes resulted in irregular cell structures and leukocytes that were often stuck together (Fig. 5c). However, lymphocytes still maintained their spherical shapes. The surface of the cell membrane was suspected to secrete mucus, and the membrane appeared folded (Fig. 5d).

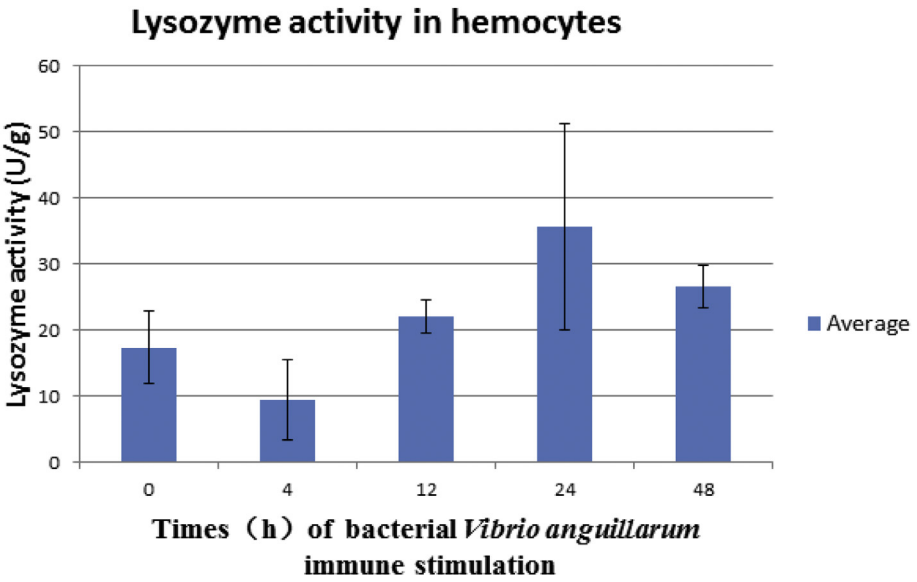


**Fig. 2.** Variation in hemocyte lysozyme activity with bacterial immune stimulation, determined using ELISA.

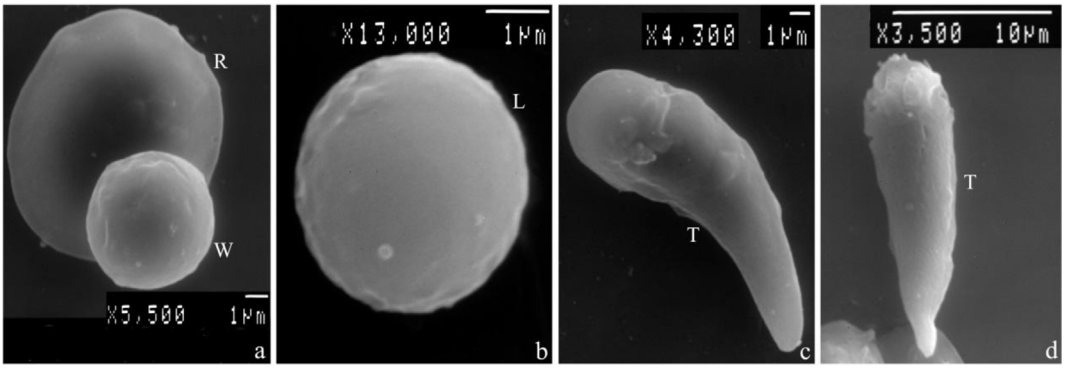


**Fig. 3.** External shape of healthy clam hemocytes.
R, red blood cell; W, white blood cell; L, lymphocyte; T, thrombocyte; a, RBC and WBC; b, lymphocyte; c and d, thrombocyte.

### 3.4. Transmission electron microscopy

Ultrastructural changes in RBCs in response to *V. anguillarum* infection are shown in Fig. 6. Fig. 6a shows a horizontal transverse section of a normal RBC and a normal leukocyte. Here, the cell membrane boundary was smooth and mellow, and the RBCs contained hemoglobin granules [1]. The WBC contained mitochondria, homogeneous cytoplasm, and an almost spherical nucleus. After *V. anguillarum* infection, hemocyte cell membranes became uneven. A longitudinally cut RBC is shown in Fig. 6b. It had swallowed a small number of *V. anguillarum* to form phagosomes at 12 h after bacterial infection. Some hemoglobin granules, small vacuoles, and an oblate nucleus were visible. The digestion and decomposition of bacteria were limited, owing to the lack of the lysosome fusion. A large number of mitochondria gathered near the nucleus after ingestion of the pathogenic bacteria. A representative phagosome containing whole and fragmented bacteria is shown in Fig. 6c. At 28 h after *V. anguillarum* infection, the blood cells digested some bacteria to form vacuoles in the cytoplasm. An erythrocyte is

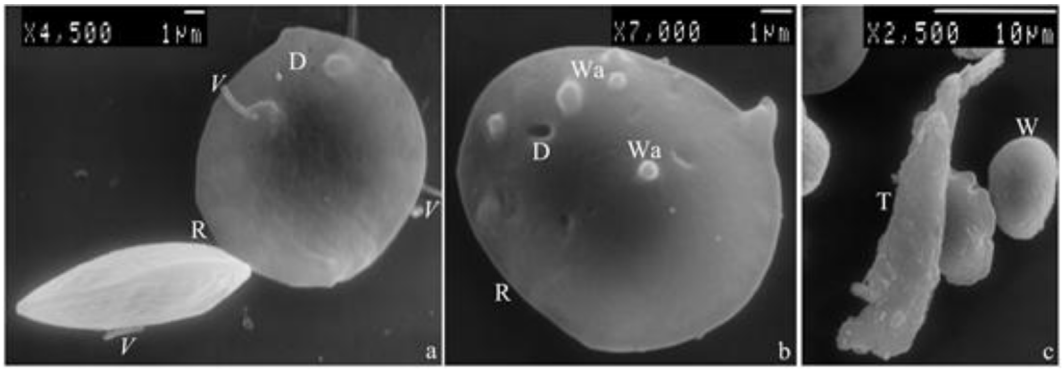


**Fig. 4.** External shape changes of red blood cell and thrombocyte after *Vibrio anguillarum* infection.
R, red blood cell; W, white blood cell; T, thrombocyte; *V*, *Vibrio anguillarum*; D, Dent; Wa, Wart.

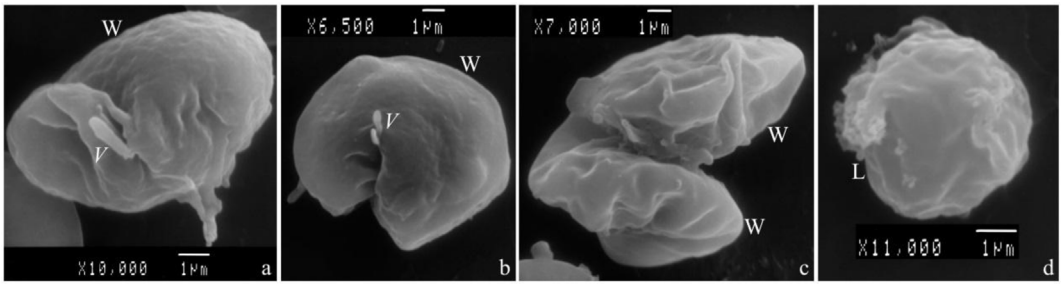


**Fig. 5.** External shape changes of white blood cell after *Vibrio anguillarum* infection.
W, white blood cell; L, lymphocyte; *V*, *Vibrio anguillarum*.

shown above, and a lymphocyte is displayed below the cell (Fig. 6d).

Ultrastructural changes in WBCs in response to *V. anguillarum* are shown in Fig. 7. WBCs displayed a strong ability to quickly kill pathogenic bacteria. WBCs could devour pathogens to form phagosomes as soon as the bacteria appeared in the hemolymph (Fig. 7a), and the phagocytic vacuole immediately fused with the lysosome to form a digestive vacuole (Fig. 7b). Several digestive vacuoles were continuously formed until the enzymes in the lysosome were depleted to form a transparent vacuole. Pathogens in the phagocytic vesicles were quickly digested into homogeneous granules, even in the transparent liquid state. A large number of mitochondria gathered near the devouring vacuoles between 8 and 28 h after *V. anguillarum* infection. It is rare to visualize the structure of bacteria devoured in WBCs, as the majority of bacteria were completely digested in the digestive vacuoles (Fig. 7c and d), unless the WBC had swallowed and digested a large number of pathogenic bacteria to form digestive vacuoles owing to the lack of lysozymes. Under these conditions, the WBC was close to death (Fig. 7e). In addition to devouring pathogens, some WBCs also phagocytized foreign objects (Fig. 7f), such as mammalian macrophages. Most WBCs had round nuclei, although some WBC nuclei were karyolobic (Fig. 7g). WBCs that phagocytized pathogens were prone to stick to each other, and special structures for adhesion were found in the

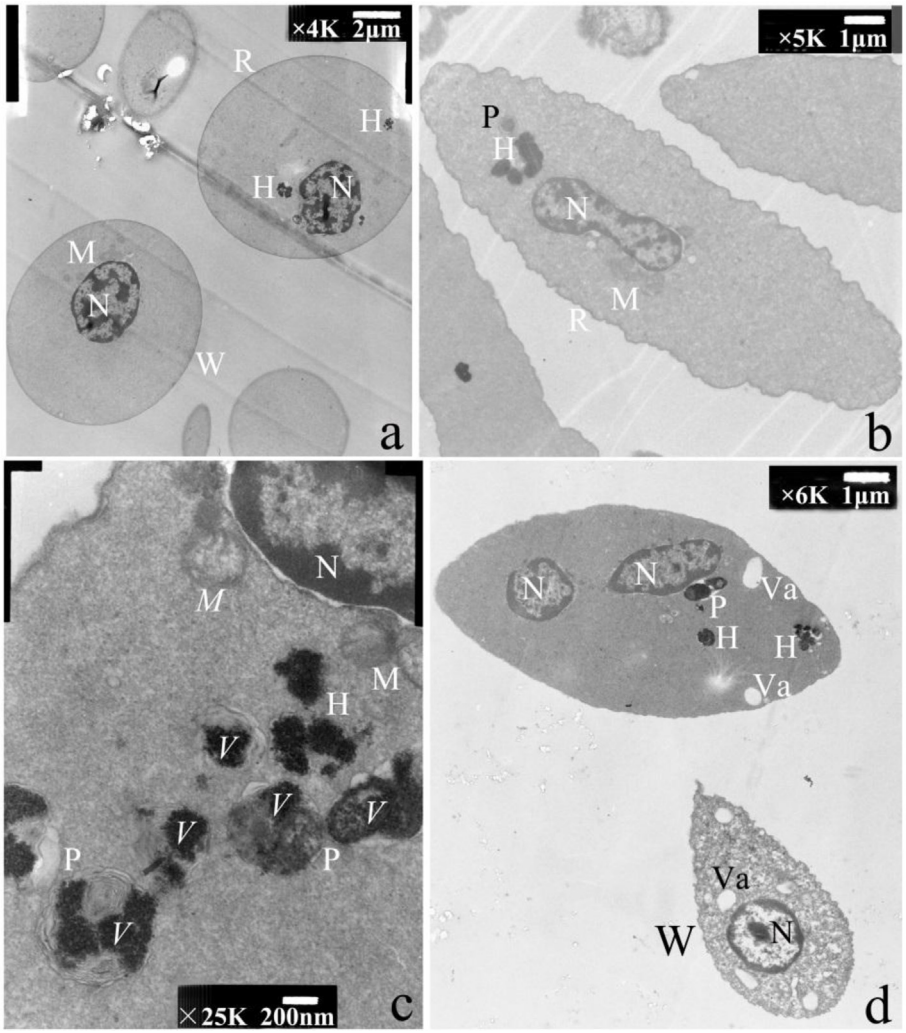


**Fig. 6.** Ultrastructural changes of red blood cells in response to *Vibrio anguillarum* infection.
R, red blood cell; W, white blood cell; H, hemoglobin granules; *V*, *Vibrio anguillarum*; M, mitochondria; P, phagosome; Va, vacuole; N, nucleus.

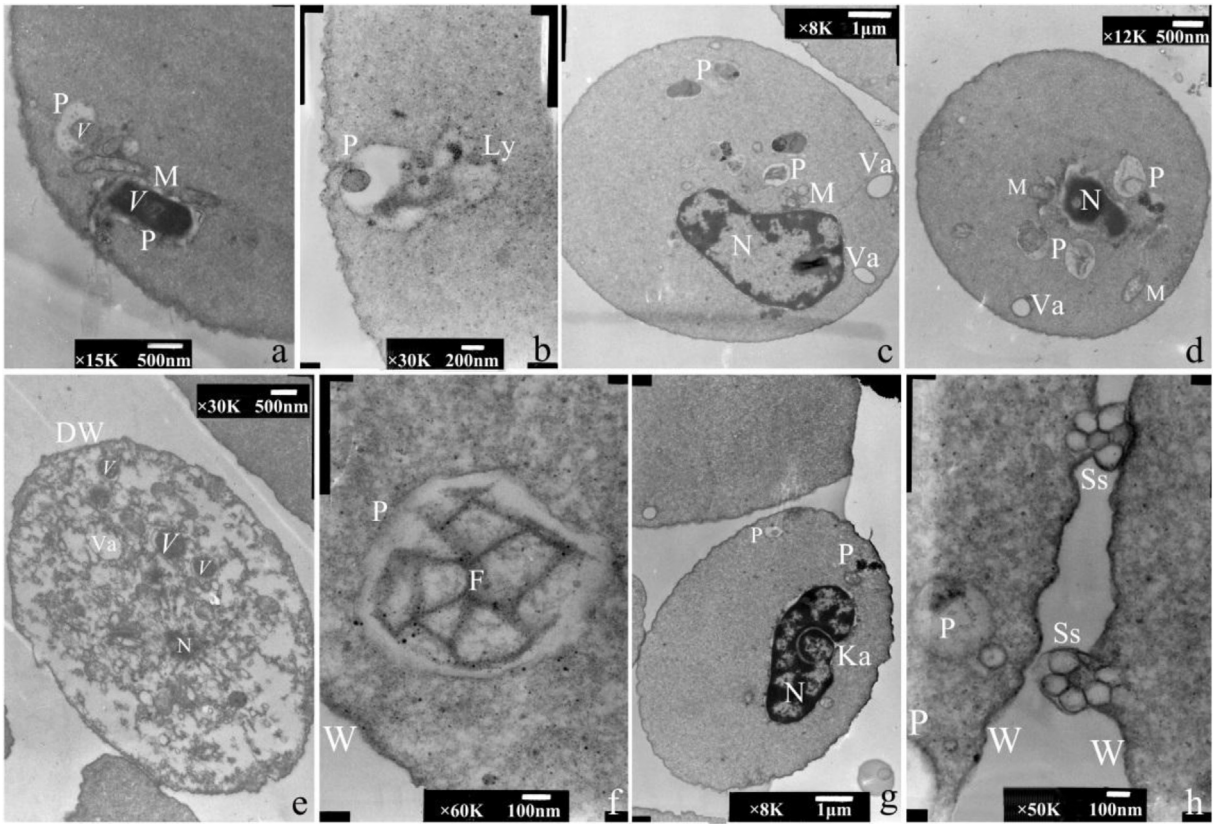


**Fig. 7.** Ultrastructural changes in white blood cell in response to *Vibrio anguillarum* infection.
W, white blood cell; H, hemoglobin granules; *V*, *Vibrio anguillarum*; M, mitochondria; P, phagosome; Va, vacuole; N, nucleus; Ss, special structure; Ly, lysosome; DW, dead WBC; F, foreign object; Ka, karyolobism.

observation (Fig. 7h).

Ultrastructural changes in TC in response to *V. anguillarum* infection are shown in Fig. 8. Although no TCs had swallowed *V. anguillarum,* as assessed by electron microscopy, the invasion of pathogenic bacteria stimulated a coagulation reaction in TCs. The TC membrane became uneven in the vicinity of blood cells that devoured pathogens. Some cytoclasis formed meshes (Fig. 8a), wherein the TCs showed huge and approximately cylindrical nuclei, cytoplasm rich in smooth-type endoplasmic reticulum (ER), and a large number of mitochondrial aggregations among the ERs (Fig. 8a, b, and c). The ER and cell membrane were constantly fused to cytoclasis. TCs initiated coagulation (Fig. 8c) and eventually formed the pseudopodia and tube-like structures to produce a mesh (Fig. 8d). The mesh structure was long enough to block cells that devoured the pathogens.

## 4. Discussion

Lysosomal hydrolytic enzymes and lysozymes in mollusk hemocytes are important elements of the defense system involved in the degradation or digestion of intrusive microorganisms [15]. Lysosomal hydrolytic enzymes are expressed in the ark shell blood plasma and hemocyte suspensions and were detected with an API ZYM kit. In the 8 and 24 h groups, all enzymes in the hemocyte suspension post *V. anguillarum* infection showed characteristics similar to those from the two diseased animals, which the hemocytes had defensive responses against *V. anguillarum* infection through variation of some hydrolytic enzyme concentrations. However, hemocytes from the 4 and 28 h groups displayed characteristics similar to those of normal individuals, and the expressed hydrolytic enzyme concentrations did not yet change remarkably or tended to be normal; no obvious changes were detected in the plasma during *V. anguillarum* infection. It was suggested that hemocytes play a more important role than plasma in the degradation and digestion of intrusive microorganisms. At 28 h after *V. anguillarum* infection, the ark shell almost recovered to its normal state, likely through cellular defenses. It is also presumed that plasma plays a role by transporting and supporting hemocytes. Lysozyme activity reached its peak in the 24 h group after *V. anguillarum* infection, as determined by ELISA. These data suggest that the lysozyme response to bacterial infection is rapid. The lysozyme activity level gradually reached to normal 48 h after *V. anguillarum* infection. Lysozyme activity levels showed great fluctuations in different individuals from the 24 h group, owing to differences in WBC counts. The higher the WBC count, the higher was the relative activity level, as lysosomes are rich in WBCs. This phenomenon was confirmed by the ultrastructural observations (Figs. 6 and 7).

Pathogen-induced changes in the ultrastructural properties of different types of hemocytes were observed by SEM and TEM. The ultrastructure function is consistent with the blood cell classification by light microscopy [4], which is remarkably different from that observed in other common cultured shellfish. Three types of hemocytes were distinguished in the flat oyster *Ostrea edulis*, including granulocytes, large hyalinocytes, and small hyalinocytes. Infection by *Bonamia ostreae* resulted in a significant increase in circulating hemocytes, mainly large hyalinocytes [16]. Large hyalinocytes have functions similar to those of WBCs in the ark shells. In this study, three well-defined hemocyte types were separated according to the morphology and functional response to *V. anguillarum* infection. RBCs are the main hemocytes involved in oxygen transport throughout the body owing to the presence of hemoglobin, while WBCs are the main hemocytes involved in cellular defense against diverse agents, such as intrusive microorganisms and foreign objects. TCs are the main hemocytes involved in blood coagulation to trap infected or dead hemocytes. The ability of hemocytes to

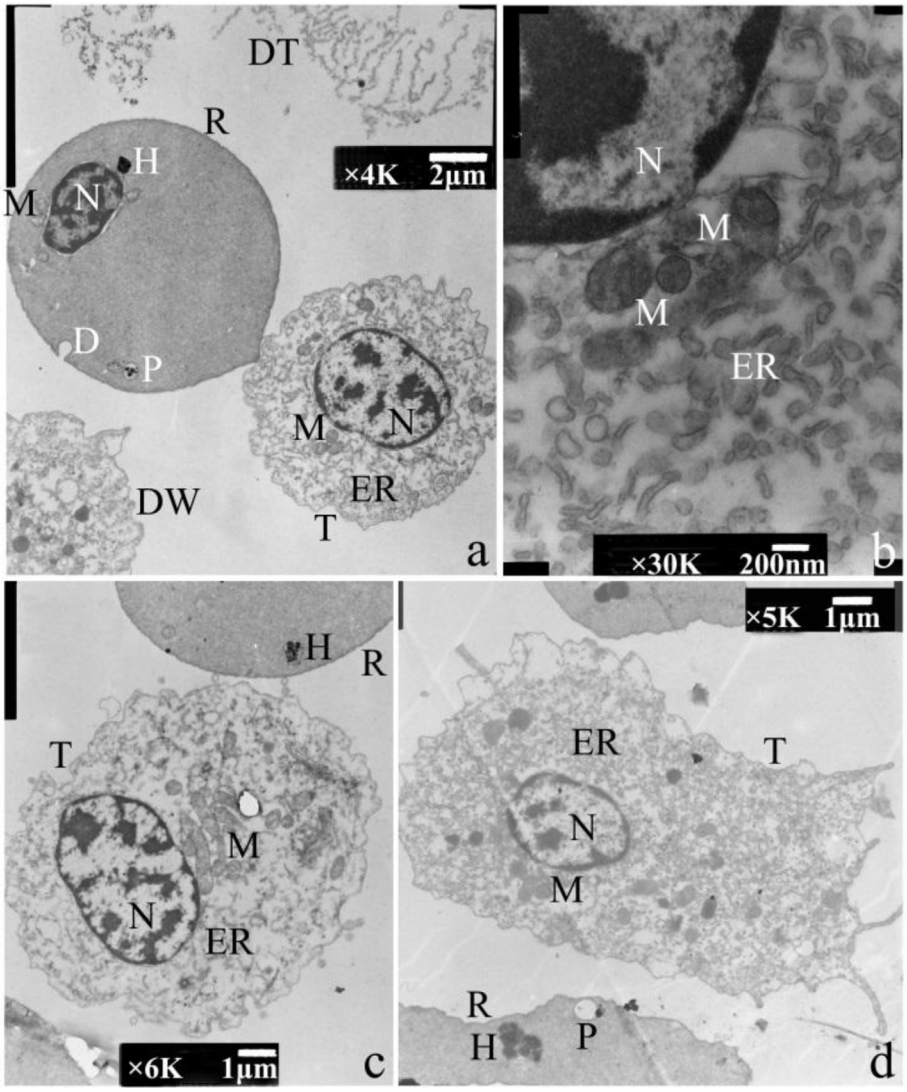


**Fig. 8.** Thrombocyte ultrastructural changes in response to *Vibrio anguillarum* infection.
R, red blood cell; T, thrombocyte; DT, Degradation of thrombocytes; H, hemoglobin granules; M, mitochondria; P, phagosome; N, nuclear; DW, dead WBC; ER, endoplasmic reticulum.

quickly change their morphologies suggests that ark shell *S. broughtonii* is endowed with different functional hemocytes to face rapid deteriorating environment as well as fast-growing pathogens.

Prior research has focused on the strong resistance of *S. broughtonii* to adverse conditions, such as low salinity, low dissolved oxygen, and pathogen infection. Almost all ark shells *S. broughtonii* used for the experiments survived throughout the experiments, including the specimens that were injected with *V. anguillarum* in the axe foot and subjected to blood withdrawal from the anterior adductor muscle sinusoid. Some special structures in the hemocytes were thought to confer this strong resistance to adversity. Hemoglobin in the RBCs functions as an iron-containing oxygen carrier and exerts antibacterial, catecholase-oxidizing [17], and phenoloxidase-like activities. Recombinant hemoglobin of *S. broughtonii* protein (rSbHb) could remarkably inhibit the growth of the gram-negative bacterium *V. anguillarum* [5]. In our study, WBCs that phagocytosed pathogens were prone to adhere to each other by some special structures, resulting in the formation of a mass that blocked wounds and prevented blood loss. This phenomenon is favorable for the amoeboid movement of WBCs. Fibronectin is presumed to be the main ingredient in these blockages, as demonstrated in the pearl oyster *Pinctada fucata*, and agranular amebocytes (hemocytes) may secrete some type(s) of cell adhesive molecules to mediate hemocyte migration to wound sites [18]. In Flannagan's view, phagocytes have a vast and sophisticated arsenal of bactericidal features, pathogens are internalized into a membrane-bound vacuole, the phagosome, which fuses with endosomes and lysosomes to become an efficient bactericidal compartment containing PI-3 kinase(s), defensins, cathelicidins, lysozymes, assorted lipases, proteases, endopeptidases, exopeptidases, and hydrolases that degrade various microbial components [19].

Thrombocytes have not yet been reported in mollusks, although little information is available on the ultrastructural characteristics of TCs in the blood of lower aquatic vertebrates. This information includes studies with trout (*Salmo gairdneri*) [20], channel catfish (*Ictalurus punctatus*) [21], turbot (*Psetta maxima*) [22], *Caiman crocodilus* yacare [23], and *Chelonia mydas* [24]; however, the structure and function of TCs were ambiguously described in these studies. Samuel Cannon observed a “fuzzy coat” in catfish TCs that covered the plasma membrane, lined the vacuoles, and distinguished TCs from lymphocytes [21]. The variability in the shape of ark shell TCs observed in the present study is supported by previous work. Burrows found that trout TCs contained numerous vesicles, ribosomes, mitochondria, Golgi complexes, ER, and a well-developed set of annular microtubules in the cytoplasm that were suggested to play an important role in determining the shape of these cells [22]. Spindle-shaped crocodile (*Caiman crocodilus yacare*)

TCs showed large nuclei with prominent heterochromatin juxtaposed to the nuclear envelope, many tubular structures and vacuoles distributed throughout the cytoplasm, and an open vesicle membrane system [23]. All of these characteristics are similar to those observed in ark shell TCs.

## 5. Conclusions

Morphological and functional changes in hemocyte sub-types were described and discussed. Hemocyte populations were able to cope with environmental changes as well as fast-growing pathogens. Plasma played a role in transporting hemocytes and supporting hemocyte structure and function. RBCs were the main hemocytes involved in oxygen transport around the body, owing to the presence of hemoglobin. WBCs were the main hemocytes involved in cellular defense against diverse stimuli, while TCs were the main hemocytes involved in blood coagulation to entrap the infected or dead hemocytes. *S. broughtonii* is endowed with highly dynamic hemocyte populations capable of coping with environmental changes and rapidly growing pathogens.

## Acknowledgments

We thank Professor Qingyin Wang for advice on experimental design and blood cell sorting. We also thank Madam Xuehong Gong for cultivating the marine unicellular alga used for feeding ark shells. This work was supported by the Central Public-interest Scientific Institution Basal Research Fund, Chinese Academy of Fishery Science (CAFS), China (NO.2018GH10), the Open Project Foundation From Key Laboratory of East China Sea & Oceanic Fishery Resources Exploitation and Utilization, Ministry of Agriculture, China (2015K02), as well as the Open Foundation from Ocean Fishery Science and Technology in the Most Important Subjects of Zhejiang province, China (20110211).

## References

[1] L.Q. Zhou, A.G. Yang, Q.Y. Wang, Z.H. Liu, B. Wu, J.T. Tian, Z.M. Lv, Studies on the hemocytes types and their immunological functions in bloody clam (*Scapharca broughtonii*), J. fish. Chin. 37 (4) (2013) 559–606.

[2] C. López, M.J. Carballal, C. Azevedo, A. Villalba, Differential phagocytic ability of the circulating haemocyte types of the carpet shell clam *Ruditapes decussatus* (Mollusca:Bivalvia), Dis. Aquat. Org. 30 (1997) 209–215.

[3] L.D. Zhou, A.G. Yang, Z.H. Liu, B. Wu, X.J. Sun, Z.M. Lv, J.T. Tian, M.R. Du, Changes in hemolymph characteristics of ark shell *Scapharaca broughtonii* dealt with Vibrio anguillarum challenge *in vivo* and various of anticoagulants *in vitro*, Fish Shellfish Immunol. 61 (2017) 9–15.

[4] L.Q. Zhou, A.G. Yang, Q.Y. Wang, Z.M. Lv, Z.H. Liu, J.T. Tian, B. Wu, Effect of *Vibrio anguillarum* on morphology and immunological function of blood cells in *Scapharca broughtonii*, Oceanol. Limnol. Sinica 45 (3) (2014) 536–541.

[5] Q. Zhao, B. Wu, Z.H. Liu, X.J. Sun, L.Q. Zhou, A.G. Yang, G.W. Zhang, Molecular cloning, expression and biochemical characterization of hemoglobin gene from ark shell *Scapharca broughtonii*, Fish Shellfish Immunol. 78 (2018) 60–68.

[6] L.B. Zheng, Z.H. Liu, B. Wu, Y.H. Dong, L.Q. Zhou, J.T. Tian, X.J. Sun, A.G. Yang, Ferritin has an important immune function in the ark shell *Scapharca broughtonii*, Dev. Comp. Immunol. 59 (2016) 15–24.

[7] L.B. Zheng, B. Wu, Z.H. Liu, J.T. Tian, T. Yu, L.Q. Zhou, X.J. Sun, A.G. Yang, A manganese superoxide dismutase (MnSOD) from ark shell, *Scapharca broughtonii*: molecular characterization, expression and immune activity analysis, Fish Shellfish Immunol. 45 (2015) 656–665.

[8] Y.H. Huang, Z.H. Liu, B. Wu, L.Q. Zhou, X.J. Sun, A.G. Yang, D.M. Li, Gene cloning and expression analysis of catalase in *Scapharca broughtonii*, J. Fish. China 40 (6) (2016) 856–866.

[9] E.S. Cho, C.G. Jung, S.G. Sohn, C.W. Kim, S.J. Han, Population genetic structure of the ark shell *Scapharca broughtonii* Schrenck from Korea, China, and Russia based on COI gene sequences, Mar. Biotechnol. 9 (2007) 203–216.

[10] J.T. Tian, Z.H. Liu, L.Q. Zhou, B. Wu, P. Liu, A.G. Yang, Isolation and characterization of 48 polymorphic microsatellite markers for the blood clam *Scapharca broughtonii* (Arcidae), Genet. Mol. Res. 11 (4) (2012) 4501–4507.

[11] M. Sekino, T. Kurokawa, K. Sasaki, Multiplex PCR panels of novel microsatellites for the ark shell *Scapharca broughtonii* (Pteriomorphia, Arcoida), Conserv. Genet. Resour. 2 (2010) 39–42.

[12] M.J. Carballal, C. López, C. Azevedo, A. Villalba, Enzymes involved in defense functions of hemocytes of mussel *Mytilus galloprovincialis*, J. Invertebr. Pathol. 70 (1997) 96–105.

[13] S.J. Chang, S.M. Tseng, H.Y. Chou, Morphological characterization via light and electron microscopy of the hemocytes of two cultured bivalves: a comparison study between the hard clam (*Meretrix lusoria*) and Pacific oyster(*Crassostrea gigas*), Zool. Stud. 44 (1) (2005) 144–153.

[14] A. Luna-González, A.N. Maeda-Martínez, F. Ascencio-Valle, M. Robles-Mungaray, Ontogenetic variations of hydrolytic enzymes in the Pacific oyster *Crassostrea gigas*, Fish Shellfish immun 16 (2004) 287–294.

[15] P. Mirella da Silva, P. Comesaña, J. Fuentes, A. Villalba, Variability of haemocyte and haemolymph parameters in European flat oyster *Ostrea edulis* families obtained from brood stocks of different geographical origins and relation with infection by the protozoan *Bonamia ostreae*, Fish Shellfish immun 24 (2008) 551–563.

[16] B. Xu, J. Zhao, Z. Jing, Y.N. Zhang, Y. Shi, T.J. Fan, Role of hemoglobin from blood clam *Scapharca kagoshimensis* beyond oxygen transport, Fish Shellfish immun 44 (2015) 248–256.

[17] T. Suzuki, S. Funakoshi, Isolation of a fibronectin-like molecule from a marine bivalve, *Pinctada fucata*, and its secretion by amebocytes, Zool. Sci. 9 (1992) 541–550.

[18] R.S. Flannagan, G. Cosío, S. Grinstein, Antimicrobial mechanisms of phagocytes and bacterial evasion strategies, Nat. Rev. Microbiol. 7 (2009) 355–366.

[19] S.S. Sekhon, H.W. Beams, Fine Structure of the developing trout erythrocytes and thrombocytes with special-reference to the marginal band and the cytoplasmic organelles, Am. J. Anat. 125 (3) (1969) 353–374.

[20] M.S. Cannon, H.H. Mollenhauer, T.E. Eurell, D.H. Lewis, A.M. Cannon, C. Tompkins, An ultrastructural study of the leukocytes of the channel catfish, *Ictalurus punctatus*, J. Morphol. 164 (1) (1980) 1–23.

[21] A.S. Burrows1, T.C. Fletcher, M.J. Manning, Haematology of the turbot, *Psetta maxima* (L.): ultrastructural, cytochemical and morphological properties of peripheral blood leucocytes, J. Appl. Ichthyol. 17 (2001) 77–84.

[22] M.W. Leal, O.L. Waldemar, E.M. Imoto, Aspectos ultraestruturales de trombocitos, eosinfilos y heterofilos de Caiman crocodilus yacare (Daudin, 1802) (Reptilia, Crocodilia), Rev. Chil. anatomía 15 (2) (1997) 201–208 Ultrastructural observations of thrombocytes, heterophils and eosinophils in Caiman crocodilus yacare (Daudin, 1802) (Reptilia, Crocodilia), Revista chilena de anatomia. 15(2) (1997) 201-208.

[23] C.L. LI, F.J. CAO, X.H. HUANG, C.W. LIU, Q.J. HUANG, Observation on the development of blood cells of *Chelonia mydas*, Oceanol. Limnol. Sinica 40 (4) (2009) 451–459.